International Journal of Remote Sensing
Vol. 28, Nos. 13–14, July 2007, 2885–2896

Taylor & Francis
Taylor & Francis Group

Multi-sensor studies of the Sumatra earthquake and tsunami of 26 December 2004

R. P. SINGH*†‡, G. CERVONE‡, M. KAFATOS‡, A. K. PRASAD§, A. K. SAHOO‡, D. SUN‡, D. L. TANG¶ and R. YANG‡

†Department of Civil Engineering, Indian Institute of Technology, Kanpur – 208016, India

‡Centre for Earth Observing and Space Research, College of Science, George Mason University, Fairfax, VA 22030, USA

§Department of Civil Engineering, Indian Institute of Technology, Kanpur 208 016, India

¶South China Sea Institute of Oceanology, Chinese Academy of Sciences, 164 West Xingang Road, Guangzhou 510301, PR China

Multi sensor satellites are now capable of monitoring the globe during day and night and provide information about the land, ocean and atmosphere. Soon after the Sumatra tsunami and earthquake of 26 December 2004, multi-sensors data have been analyzed to study the changes in ocean, land, meteorological and atmospheric parameters. A pronounced changes in the ocean, atmospheric and meteorological parameters are observed while comparing data prior and after the Sumatra main event of 26 December 2004. These changes strongly suggest a strong coupling between land, ocean and atmosphere associated with the Sumatra event.

1. Introduction

A mega-earthquake (M_w=9.3; epicentre: latitude 3.30° N and longitude 95.7° 8E, and focal depth 10 km) occurred off the coast of Sumatra on 26 December 2004. This earthquake was one of the largest and most destructive earthquakes to have occurred in the past 100 years. The event caused a tsunami that affected the coastal regions of several countries, India, Indonesia, Malaysia, Maldives, Myanmar (Burma), Sri Lanka, and Thailand, and even Somalia and Kenya in far-away Africa. This earthquake event and associated tsunami caused changes on the land and in the oceans, atmosphere, and ionosphere.

Numerous satellites orbit in space and cover the whole globe. Earthquakes occur on land and in the oceans, and the effects are felt by people living on the Earth. Earthquakes occurring on land and in the ocean give rise to changes in the ocean and on the land, and such changes have been observed prior to earthquakes. Solid-earth geophysicists and seismologists have made efforts in the past to determine the complementary behaviour of surface and subsurface parameters associated with the earthquakes measured from the ground using shallow and deeper geophysical techniques. All these observations have failed to show any strong evidence or one-to-one relation either prior or after an earthquake, due to numerous limitations.

*Corresponding author. Email: rsingh3@gmu.edu

International Journal of Remote Sensing
ISSN 0143-1161 print/ISSN 1366-5901 online © 2007 Taylor & Francis
http://www.tandf.co.uk/journals
DOI: 10.1080/01431160701237405

One such major limitation has been the lack of continuous observations. With the numerous satellites in orbit capable of continuous monitoring of land, ocean, atmosphere, and ionosphere parameters, strong evidence of changes in land, ocean, atmosphere, and ionosphere parameters associated with earthquakes has been observed (Dey and Singh 2003, Dey *et al.* 2004, Cervone *et al.* 2004, Okeda *et al.* 2004, Ouzounov and Freund 2004, Trigunait *et al.* 2004, Singh *et al.* 2001a, b, 2002, 2006). The remote sensing data has also been widely used in the mapping of damage due to the Gujarat earthquake (Singh *et al.* 2001c, Yusuf *et al.* 2001).

Changes in land, oceanic, and atmospheric parameters have also been observed prior to large earthquakes using remote-sensing data. These changes suggest the existence of a strong coupling between land, ocean, atmosphere, and ionosphere associated with earthquake processes. Recent studies using remote-sensing data have shown that such strong coupling is associated with the build-up of stress in the earthquake hypocentral region (Dey and Singh 2003, Cervone *et al.* 2004, Pulinets *et al.* 2006). The analysis of multi-sensor data has shown that the associated parameters change significantly with earthquakes of magnitude 5.5 and greater with a focal depth up to 35 km (Dey and Singh 2003, Cervone *et al.* 2004, 2005, Singh *et al.* 2006).

In the present paper, changes before and after the Sumatra earthquake on the land, ocean, and atmosphere based on the analysis of multisensor parameters are discussed. These changes show a complementary behaviour in terms of the various land, ocean and atmospheric parameters, further showing strong evidence of coupling between land, ocean, and atmosphere associated with the Sumatra earthquake of 26 December 2004.

2. Multi-sensor satellite parameters

Satellites are capable of observing the land, ocean, atmosphere, and ionosphere day and night, and during cloud and clear sky conditions, at high spatial and temporal resolutions in the broad-wavelength electromagnetic spectrum. We have analysed surface latent heat flux, wind, water vapour, sea surface temperature, and chlorophyll concentrations. All these parameters are derived from satellite data and are freely available. Sea surface temperature (SST), atmospheric water vapour (WV), cloud liquid water (CLW), and precipitation rate (PR) data were obtained from the Tropical Rainfall Measuring Mission (TRMM) Microwave Imager (TMI) (http://www.ssmi.com). The resolution of TMI data ranges from 5 km at 85.5 GHz to 45 km at 10.65 GHz (Kummerow *et al.* 2000). The surface latent heat flux (SLHF) data were taken from http://iridl.ldeo.columbia.edu/SOURCES/.NOAA/.NCEP-NCAR/. The data set is in the form of a global grid of $1.8^\circ \times 1.8^\circ$ resolution. A validation and detailed description of the reanalysis of NCEP SLHF data have been discussed by Kalnay *et al.* (1996). SLHF estimation depends on various geophysical parameters such as SST, water vapour (WV), and wind speed (WS) (Schulz *et al.* 1997). The dependence of SLHF on the above parameters can be obtained from the following equation:

$$Q_l = \rho L_E C_L u(q_s - q_a), \tag{1}$$

where the subscript a corresponds to a reference altitude, s denotes surface quantities, C_L denotes the bulk transfer coefficient, q is the specific humidity, u *is* the scalar wind, and ρ and L_E are constants.

The anomalies are obtained by subtracting the multi-year mean from the area-averaged values and divided by multi-year mean values, which can be expressed as:

$$\text{Anomaly} = [(\text{value} - \text{mean})/\text{std. deviation}] \times 100\%. \quad (2)$$

The Chl *a* data (level-3) is derived from MODIS (spatial resolution, 4 km) onboard the Aqua spacecraft of the Earth Observing System (EOS) (2004–2005). The data processing is carried out by $\log_{10}$ transformation (logarithm transformation which uses the base 10 logarithm function to provide a better visualization), and images are generated using MATLAB v. 6.5 and the Grid Analysis and Display System (GrADS) v. 1.8.

3. Results and discussion

Figure 1 shows a topographical map with the continental boundaries, major fault lines, and epicentres of earthquakes (of magnitude larger than 5), which occurred

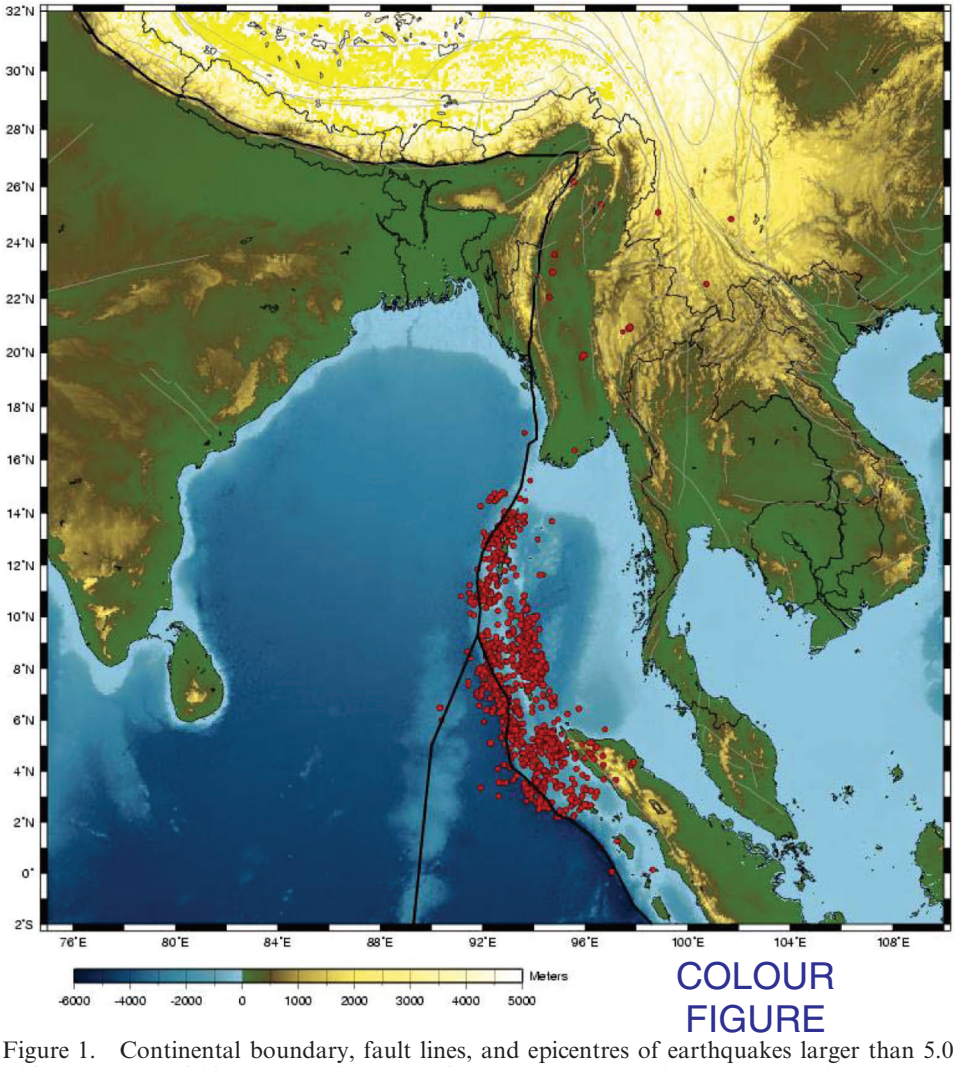

Figure 1. Continental boundary, fault lines, and epicentres of earthquakes larger than 5.0 which occurred within a week after the main Sumatra earthquake of 26 December 2004.

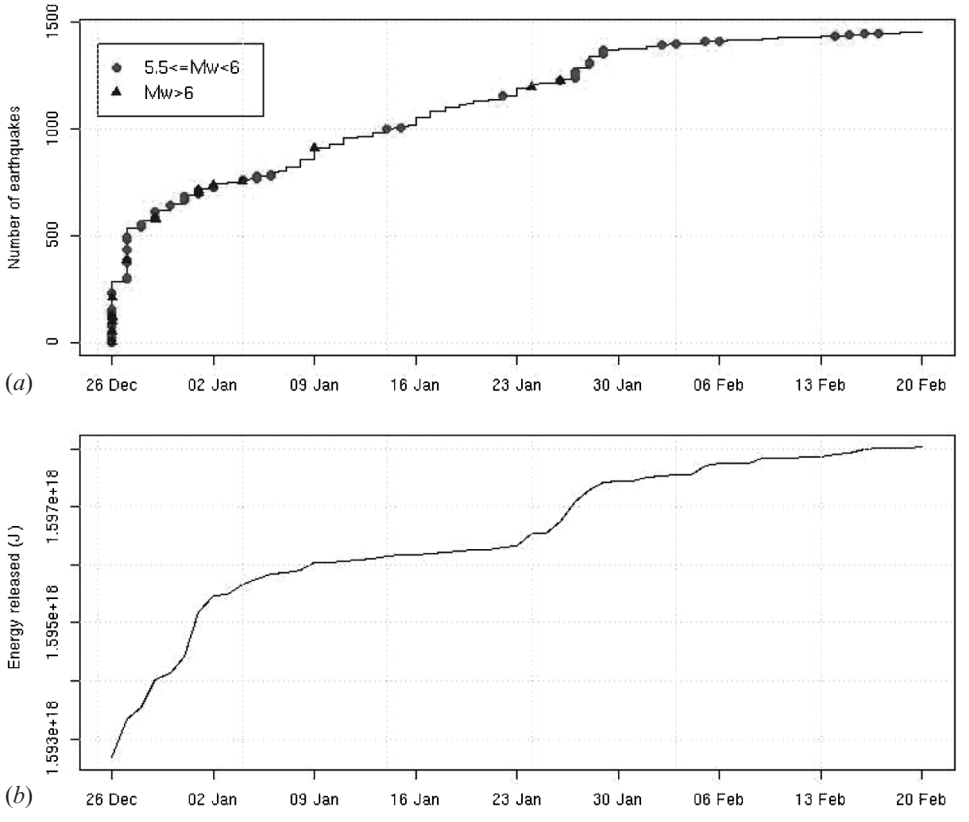

Figure 2. Cumulative number of earthquakes and energy released 2 months after the main event.

within a week after the main event of 26 December 2004. The main earthquake event caused a rupture in an area up to about 1000 km long and 100 km wide, which is inferred from the location of aftershocks. Within 2 months of the main earthquake event, over 1500 earthquakes had occurred, releasing an energy roughly equal to 1.6×10^{18} J. About 90% of this energy was released from the main earthquake of 26 December 2004 (M_w=9.3). Figure 2 shows the cumulative number of earthquake events and the energy released as a function of time.

3.1 *SLHF, SST, WV, PR, and CLW anomalies*

The SLHF data over the Indian Ocean show strong SLHF anomalies lasting several (~10) days, over several grids of size 200 km × 200 km. The strong SLHF anomaly is observed first on 7 December 2004 near the Andaman and Nicobar islands and again on 12 March near Sumatra. The SLHF maxima were observed on 7 December, far from the epicentre of the main earthquake at the intersection of the Java trench and 90° east ridge figure 3(*a*). For this strongest earthquake in the past 100 years, it is very likely that there may have been heating over a larger region due to the large stress associated with this large earthquake. In fact, the large extent of the activities is corroborated by the large-scale spatial distribution of aftershocks. Perhaps for this mega-earthquake, stresses occurred over very large regions, up to

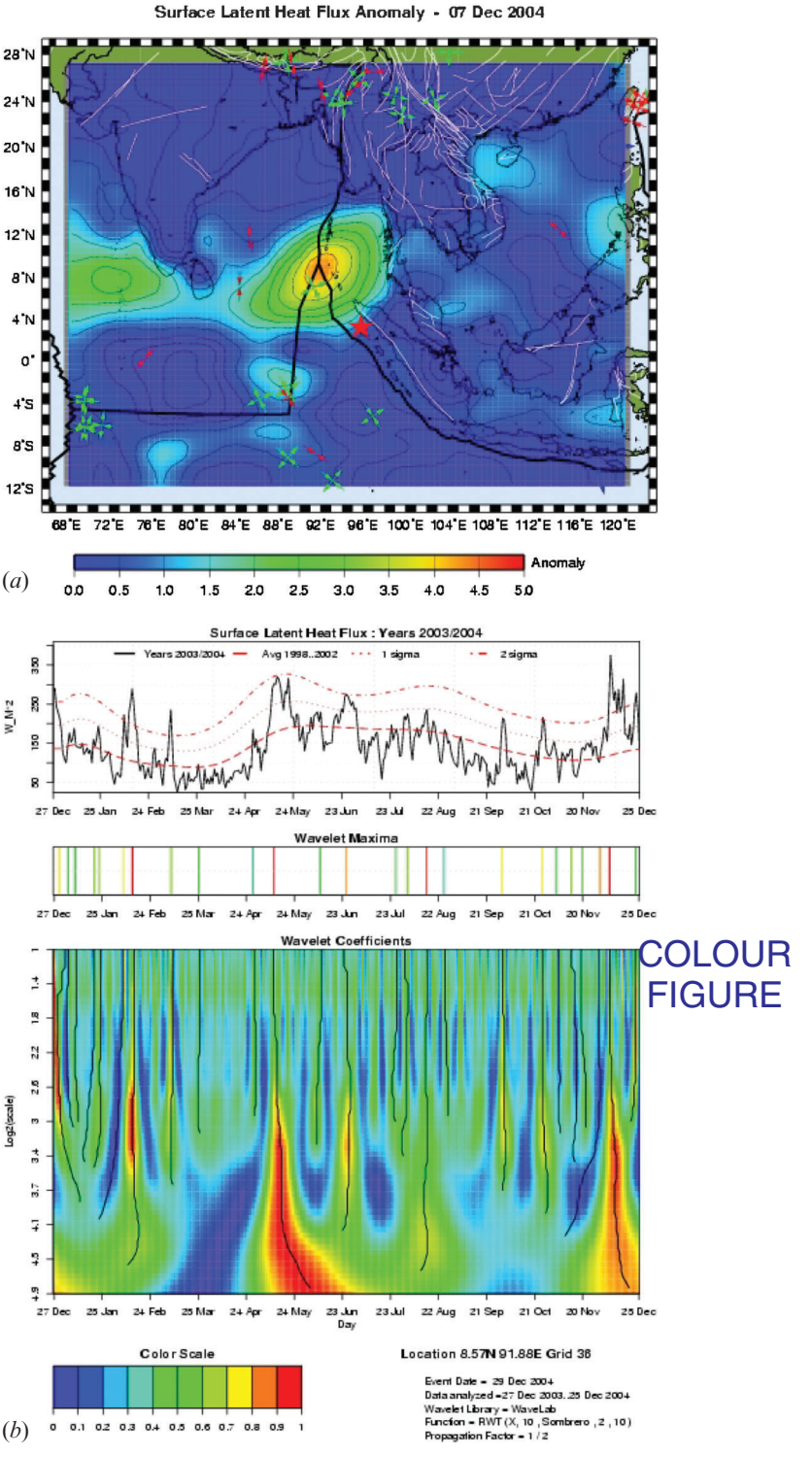

Figure 3. (*a*) SLHF anomaly on 7 December 2004. (*b*) Time series of wavelet analysis of SLHF for the period from 27 December 2003 to 25 December 2004.

more than 1000 km, while the location where the rupture occurred is more random and is likely related to the fault geometry. Within the observed changes on land, ocean, atmosphere, and ionosphere after the earthquakes, SLHF is found to be one of the important parameters related to the heat budget of the Earth. The coupling between land, ocean, and atmosphere causes anomalous SLHF values prior to large coastal earthquakes. Very strong SLHF anomalies were observed prior to the 26 December 2004 earthquake, which are localized in time and space over the epicentral region and along the tectonic plate boundaries.

Figure 3(*b*) shows the temporal behaviour of SLHF for 1 year, giving the time history for the region of maximum anomaly, and a decomposition of the signal in different scales using a real wavelet transformation. The anomaly associated with the 26 December 2004 event is found to be the largest during the time period, and also the largest in the past 5 years. The wavelet decomposition shows that the SLHF anomaly observed on 7 December 2004 has high coefficients at all scales, a characteristic that has been observed for most anomalies associated with coastal earthquakes.

Figure 4 shows SLHF anomaly variations along latitude -5° to $+18^\circ$ N for the period December 2004–April 2005. All earthquakes greater than magnitude 5 are shown with black circles, with the size of the circles showing the magnitude of the earthquake. The largest circle on 26 December 2004 shows the main earthquake event.

The mean SST anomaly for 7 years (1998–2004) shows an anomalous increase (more than 1° C) over a large area of ocean to the west of the epicentre of the main earthquake prior to the earthquake (23–25 December 2004) (figure 5(*a*)). This may be because of the enhanced IR emission from the Earth's surface in the 8–12 μm region; such a high IR emission was also observed in the Gujarat earthquake (Ouzounov and Freund 2004). The high SST anomaly coincides with the high SLHF

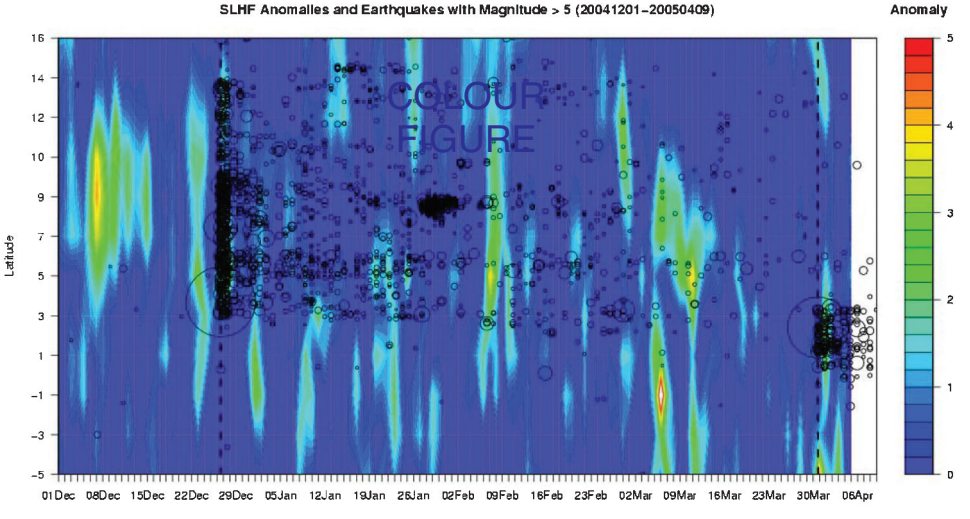

Figure 4. Latitude–time display of SLHF with times and latitudes of earthquake events shown as black circles. Black circles show the epicentres of earthquakes, and the size of the circle represents the magnitude of earthquakes. All earthquake aftershocks higher than 5.0 are shown.

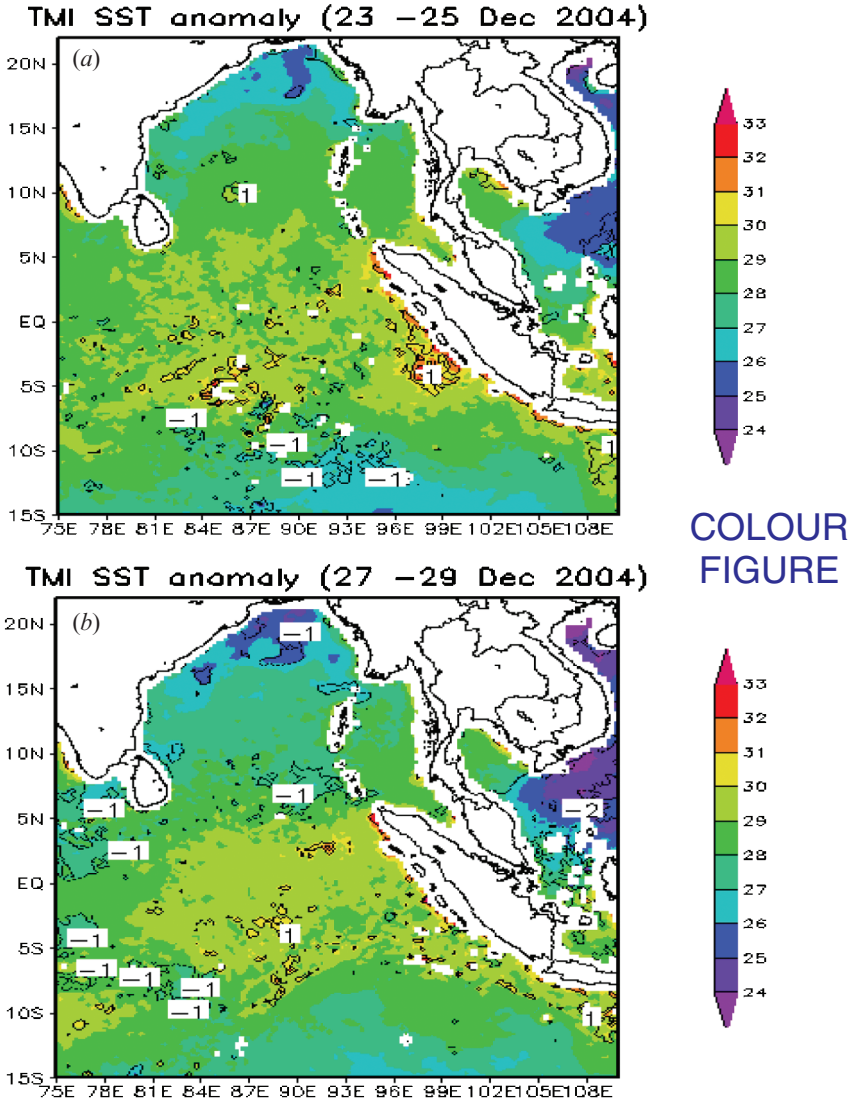

Figure 5. SST (shaded) and anomaly (contour) from a 7-year mean (1998–2004) (contour) for: (*a*) before the earthquake (23–25 December 2004) and (*b*) after the earthquake (27–29 December 2004).

anomaly on 7 December 2004 (figure 3(*a*)); this is because the SLHF is strongly affected by the SST over ocean. Equation (1) shows the relationship between SST and SLHF that supports this observation. The increase in SST before and after the earthquake, led to an increase in energy exchange between ocean and atmosphere, and as a result a high SLHF anomaly was found prior to the earthquake. After the main event (27–29 December 2004), the SST was found to decrease by more than 1°C along the west coast of the Andaman and Nicobar Islands (figure 5(*b*)).

The SST shows a strong increase from 6 to 8 December 2004 (figure 6), followed by a decrease from 24 December prior to the main earthquake, and reached the lowest on 29 December, afterwards returning to the background SST value. The

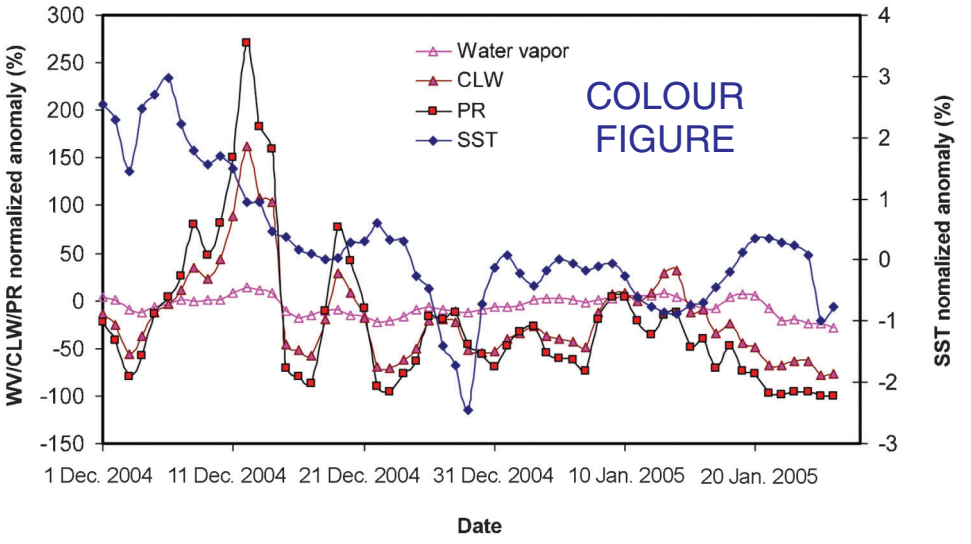

Figure 6. Time series of CLW averaged over the west coast of Sumatra (5–10° N, 90–100° E) from 1 December 2004 to 31 January 2005.

SST and SLHF were both found to show an anomalous increase prior to the earthquake from 6 to 8 December 2004. Various other parameters such as WV, PR, CLW, and SST averaged over the west coast of Sumatra (5–10° N, 90–100° E) showed one-to-one correlations of WV and CLW and of CLW with PR. However, no noticeable changes associated with the main earthquake event were found. The correlations and *t*-test results are given in table 1.

3.2 *Changes in wind direction*

The analysis or daily mean wind data (u and v wind, horizontal wind vectors), obtained from National Center for Environmental Prediction (NCEP) reanalysis, has been carried out to study the changes in the wind field at three pressure levels (850, 500 and 200 mb) during 24–28 December 2004. A similar analysis has been carried out using the NCEP wind data for the years 2001–2003 for the same time period (24–28 December), and no significant changes in wind direction have been found. The wind speed was found to increase by 50–100% after the tsunami at 850 and 200 mb pressure levels, whereas a decrease in wind speed by 50–100% was observed at a pressure level of 500 mb. Such changes in wind speed are not unique when compared to earlier years. The wind data for 24–28 December for the year 2004 show pronounced changes in wind direction after the tsunami event over the ocean as well as on the land. The statistical test (Davis 2002) for comparison of the wind direction on 25 and 27

Table 1. Correlation and *t*-test results between atmospheric water vapor (WV) and cloud liquid water (CLW), cloud liquid water and precipitation rate (PR).

	R	*P*-value	df
WV/CLW	0.59	0.00008	112
CLW/PR	0.96	0.078	112

R represents the correlation coefficient. The *P*-value is the *t*-test result, and df refers to the degree of freedom.

December 2004 (1 day before and after the tsunami) shows significant changes at all pressure levels by more than 40–90° over the Indian Ocean (0–5° N and 85–95° E) and the Bay of Bengal (10–15° N and 85–95° E) (see figure 7).

3.3 *Changes in GPS water vapour*

The continuous hourly profile of precipitable water vapour derived from over two International GNSS (Global Navigation Satellite System) Service (IGS) Global Positioning System (GPS) stations (NTUSGPS 1.34° N 103.67° E, Nanyang Technological University, Singapore; and BAKO 6.49° S 106.85° E, Bakosurtanal, Cibinong city) which are close to the epicentre of the Sumatra Earthquake show anomalous behaviour where the column water vapour is found to be low by a large extent (over 3σ) (figure 8). The detrended GPS water vapour is obtained by subtracting the 24-h running average of water vapour from individual hourly recordings. A large decrease by over 3σ is observed 10–12 days prior to the earthquake event over NTUS and BAKO stations (figure 8). This anomalous deviation of water vapour ($>3\sigma$) is found to be more prominent over the station closer to the epicentre (NTUS) compared to station BAKO and other GPS stations far away from the epicentre.

3.4 *Changes in chlorophyll a concentration*

An anomalous increase in chlorophyll *a* (Chl *a*) concentration was observed soon after the Gujarat earthquake (Singh *et al.* 2006). Increase in chlorophyll

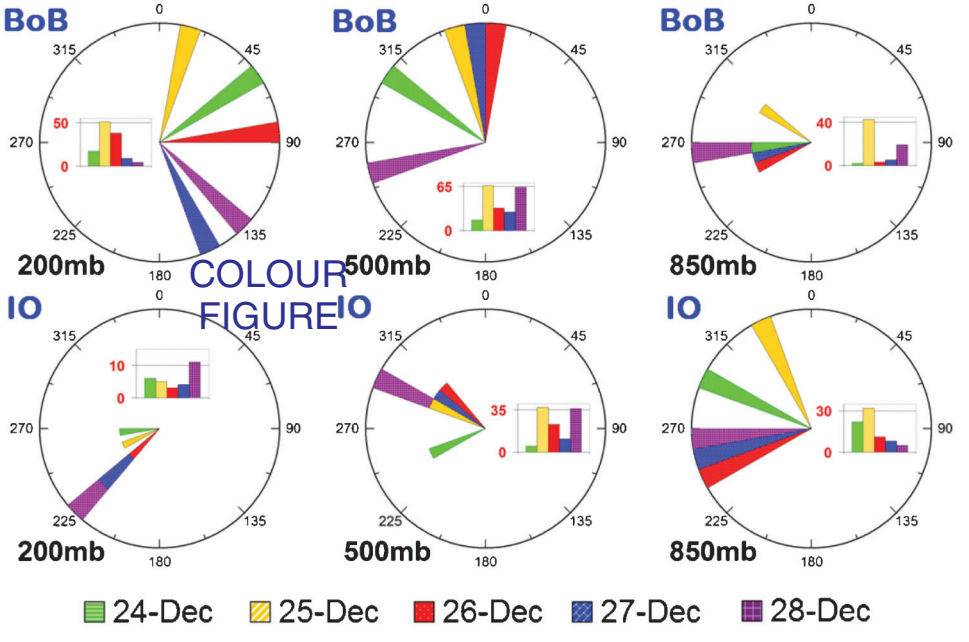

Figure 7. Change in wind direction from 24 to 28 December 2004. BoB: Bay of Bengal; IO: Indian Ocean. The histogram inside the rose diagram gives the 95% confidence interval of the mean direction (±). Mean directions are plotted as a 10° interval. The radius of the rose diagram does not indicate the magnitude of the wind. Overlapping angles are presented as stacked sectors.

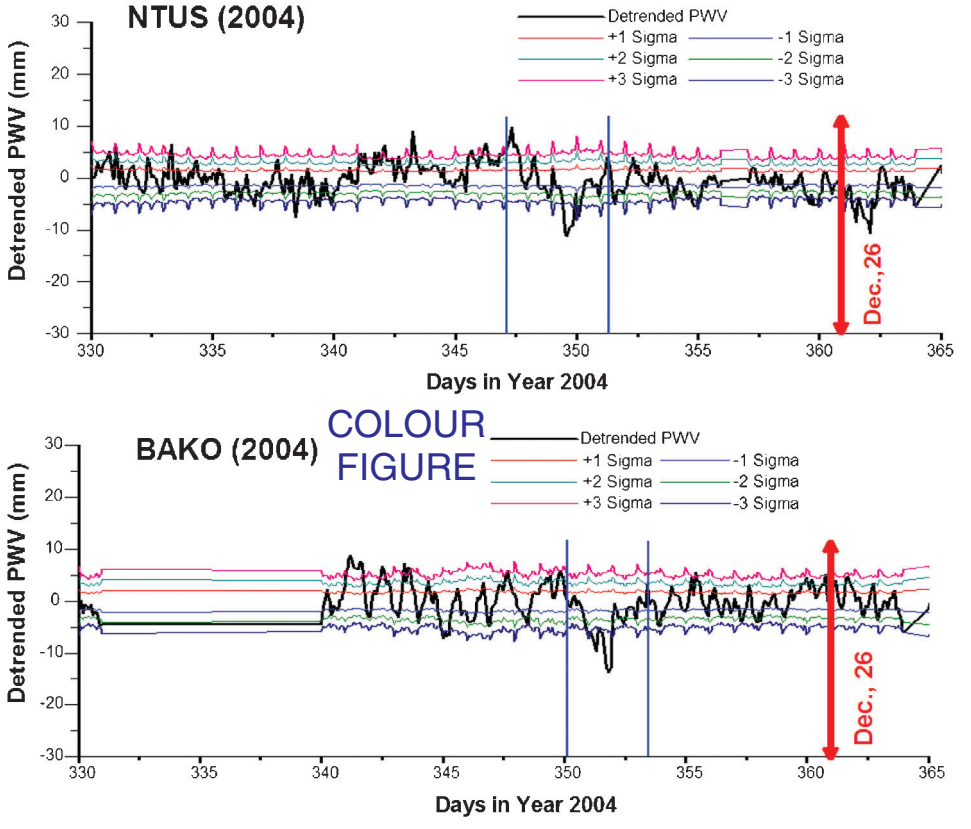

Figure 8. GPS water-vapour hourly profile over IGS GPS stations NTUS and BAKO after subtracting the 24-h running average from individual readings showing anomalous and large changes in column water vapour about 10–12 days prior to the main event (26 December 2004).

concentration was also found in a few coastal earthquakes (Singh *et al.* 2006). Soon after the Sumatra earthquake, daily concentrations of Chl *a* from MODIS data were analysed over the area covered by longitude 91–96° E and latitude 4–9° N. High Chl *a* concentrations were found prior to the two earthquakes of 26 December 2004 and 28 March 2005 (figure 9). After the main earthquake of 26 December 2004, a number of earthquake aftershocks of varying magnitudes occurred. The high concentrations of Chl *a* seem to correspond to the earthquake aftershocks of magnitude greater than 5.5. The Chl *a* concentration was found to increase prior to the earthquake (up to 0.3 mg m^{-3}) on 22 December 2004 (figure 9), and subsequently Chl *a* was found to decrease for 1 week during the tsunami and to increase again afterwards (2 in figure 9). A similar trend was also observed during March 2005, with two maxima peaks of Chl *a* (3 and 4, figure 9) associated with the earthquake of 28 March 2005. Generally, the Chl *a* concentration was found to be high during the period December 2004 to March 2005 (line T, figure 9).

4. Conclusions

In summary, SST is found to increase anomalously before the earthquake (6–8 December), decrease anomalously prior to and soon after the earthquake (24–29

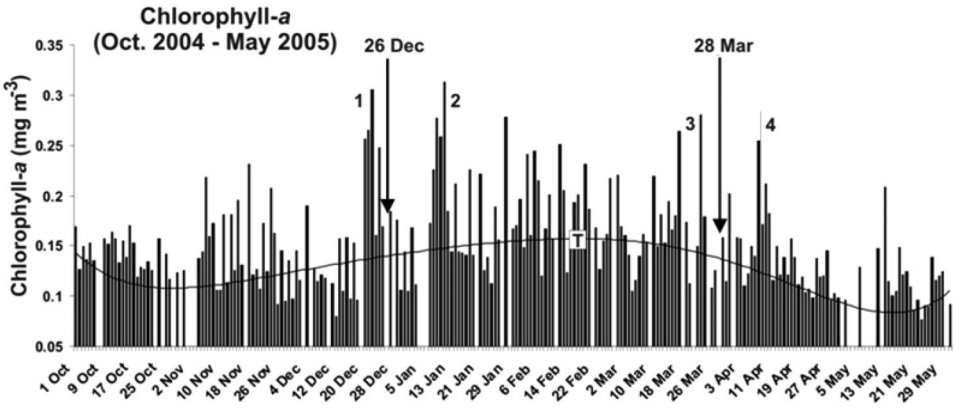

Figure 9. Variability of chlorophyll *a* concentration during October 2004 to May 2005 over an area bounded by longitude 91–96° E and latitude 4–9° N.

December), and to recover its normal value 5 days after the earthquake. Due to the increase in surface winds and SST, the SLHF is found to increase anomalously on 7 December 2004 to the west of the epicentre of the main Sumatra earthquake. Because of the increase in SLHF and ocean–atmosphere interaction, WV, CLW, and PR over the ocean west of Sumatra are found to increase prior to the earthquake (12 December 2004). The anomalous changes in oceanic and atmospheric parameters were found to be related. The atmospheric anomalies were found to lag qualitatively with the ocean surface variables and found to be more significant compared to the surface anomalies. Our results clearly show qualitative changes. This work may be the first step in the development of a quantitative basis for assessing the anomalies and consequences due to the changes associated with the ocean and atmosphere interaction induced by earthquakes.

Acknowledgements

RPS is grateful to the Department of Science and Technology, New Delhi for the financial support under which GPS data analysis was supported. Part of the work was supported by a grant 'The National Natural Science Foundation of China (NSFC40576053)' awarded to DT. The authors are grateful to Professor Arthur Cracknell for providing comments and suggestions that have helped us to improve this paper.

References

CERVONE, G., KAFATOS, M., NAPOLETANI, D. and SINGH, R.P., 2004, Wavelet maxima curves associated with two recent Greek earthquakes. *Natural Hazards and Earth System Sciences*, **4**, pp. 359–374.

CERVONE, G., SINGH, R.P., KAFATOS, M. and YU, C., 2005, Wavelet maxima curves of surface latent heat flux anomalies associated with Indian earthquakes. *Natural Hazards and Earth System Sciences*, **5**, pp. 87–99.

DAVIS, J.C., 2002, *Statistics and Data Analysis in Geology*. 3rd ed. Wiley, New York.

DEY, S., SARKAR, S. and SINGH, R.P., 2004, Anomalous changes in column water vapor after Gujarat earthquake. *Advances in Space Research*, **33**, pp. 274–278.

DEY, S. and SINGH, R.P., 2003, Surface latent heat flux as an earthquake precursor. *Natural Hazards and Earth System Sciences*, **3**, pp. 749–755.

KALNAY, E., KANAMITSU, M., KISTLER, R., COLLINS, W., DEAVEN, D., GANDIN, L., IREDELL, M., SAHA, S., WHITE, G., WOOLLEN, J., ZHU, Y., LEETMAA, A., REYNOLDS, B., CHELLIAH, M., EBISUZAKI, W., HIGGINS, W., JANOWIAK, J., MO, K.C., ROPELEWSKI, C., WANG, J., JENNE, R. and JOSEPH, D., 1996, The NCEP/NCAR 40-year reanalysis project. *Bulletin of the American Meteorological Society*, **77**, pp. 437–471.

KUMMEROW, C., SIMPSON, J., THIELE, O., BARNES, W., CHANG, A.T.C., STOCKER, E., ADLER, R.F., HOU, A., KAKAR, R., WENTZ, F., ASHCROFT, P., KOZU, T., HONG, Y., OKAMOTO, K., IGUCHI, T., KUROIWA, H., IM, E., HADDAD, Z., HUFFMAN, G., FERRIER, B., OLSON, W.S., ZIPSER, E., SMITH, E.A., WILHEIT, T.T., NORTH, G., KRISHNAMURTI, T. and NAKAMURA, K., 2000, The status of the Tropical Rainfall Measuring Mission (TRMM) after two years in orbit. *Journal Applied Meteorology*, **39**, pp. 1965–1982.

OKADA, Y., MUKAI, S. and SINGH, R.P., 2004, Changes in atmospheric aerosol parameters after Gujarat earthquake of January 26, 2001. *Advances in Space Research*, **33**, pp. 254–258.

OUZOUNOV, D. and FREUND, F., 2004, Mid-infrared emission prior to strong earthquakes analyzed by remote sensing data. *Advances in Space Research*, **33**, pp. 268–273.

PULINETS, S.A., OUZOUNOV, D., CIRAOLO, L., SINGH, R., CERVONE, G., LEYVA, A., DUNAJECKA, M. and KOTSARENKO, A., 2006, Thermal, atmospheric and ionospheric anomalies around the time of the Colima M7.8 earthquake of 21 January 2003. *Annales Geophysicae*, **24**, pp. 835–849.

SCHULZ, J., MEYWERK, J., EWALD, S. and SCHLUSSEL, P., 1997, Evaluation of satellite-derived latent heat fluxes. *Journal of Climate*, **10**, pp. 2782–2795.

SINGH, R.P., SAHOO, A.K., BHOI, S., KUMAR, M.G. and BHUIYAN, C., 2001a, Ground deformation of the Gujarat earthquake of 26 January 2001. *Journal of the Geological Society of India*, **58**, pp. 209–214.

SINGH, R.P., BHOI, S., SAHOO, A.K., RAJ, U. and RAVINDRAN, S., 2001b, Significant changes in ocean parameters after Gujarat earthquake. *Current Science*, **80**, pp. 101–102.

SINGH, R.P., BHOI, S. and SAHOO, A.K., 2001c, Surface manifestations after the Gujarat earthquake. *Current Science*, **80**, pp. 1376–1377.

SINGH, R.P., BHOI, S. and SAHOO, A.K., 2002, Changes observed in land and ocean after Gujarat earthquake of January 26, 2001 using IRS data. *International Journal of Remote Sensing*, **23**, pp. 3123–3128.

SINGH, R.P., DEY, S., BHOI, S., SUN, D., CERVONE, G. and KAFATOS, M., 2006, Anomalous increase of chlorophyll concentrations associated with earthquakes. *Advances in Space Research*, **37**, pp. 671–680.

TRIGUNAIT, A., PARROT, M., PULINETS, S.A. and LI, F., 2004, Variations of the ionosphere electron density during the Bhuj seismic event. *Annales Geophysicae*, **22**, pp. 4123–4131.

YUSUF, Y., MATSUKO, M. and YAMAZAKI, F., 2001, Damage assessment after 2001 Gujarat earthquake using Landsat-7 Satellite Images. *Journal of the Indian Society of India*, **29**, pp. 17–22.